IMPACT DEMAGNETIZATION AT MARS: NEW CONSTRAINTS FROM MONTE CARLO MODELING AND MULTIPLE ALTITUDE MAGNETIC FIELD DATA.

Robert J. Lillis[1] (rlillis@ssl.Berkeley.edu), Jasper S. Halekas[1], Sarah T. Stewart[2], Karin L. Louzada[2,3], Michael E. Purucker[4], Michael Manga[5]

[1]UC Berkeley Space Sciences Laboratory, 7 Gauss Way, Berkeley, CA 94720 UC Berkeley

[2]Harvard University Department of Earth and Planetary Sciences, 20 Oxford St., Cambridge, MA 02138.

[3]Netherlands Office for Science & Technology, Netherlands Embassy, 4200 Linnean Ave NW, Washington, D.C.

[4]Planetary Geodynamics Laboratory, NASA Goddard Space Flight Center, Greenbelt, MD 20771

[5]UC Berkeley Department of Earth and Planetary Sciences, McCone Hall, Berkeley, CA 94720

Introduction: The magnetic field signatures of large demagnetized impact basins on Mars offer a unique opportunity to study the magnetic properties of the crust and the processes of basin formation and impact shock demagnetization [1, 2]. We present a framework for determining the effects on such signatures due to the dominant direction, strength, thickness and vertical and horizontal coherence wavelengths of the surrounding crustal magnetization, as well as the demagnetization radius and the width of the linear demagnetization gradient zone caused by impact shock.

Magnetic field data at 2 altitudes are taken from the Mars Global Surveyor mission: magnetic field magnitudes at 185 km from electron reflectometry [3] (B_{185}) and an internal magnetic field model of Mars based on magnetometer measurements and the technique of Purucker [4], evaluated at 400 km altitude (B_{400}). Having multiple altitude data helps us to characterize the altitude decay of the magnetic field, and hence constrained quantities such as the coherence wavelength of the magnetization.

Fourier domain stochastic modeling of impact demagnetization signatures: to avoid the nonuniqueness inherent in inverse modeling of specific magnetic sources, we take a statistical approach and model the magnetic field observed over a cylindrically uniform demagnetized impact basin where the surrounding crustal magnetization is a random Gaussian distribution filtered in Fourier space to have different Gaussian distributions in vertical and horizontal coherence wavelength. The overall layer thickness is 48 km. We constructed a large database of radial profiles of circumferential averages of magnetic field magnitude at 0 km and 30 km for ranges of the following parameters:

1) strength, 2) direction, 3) vertical coherence wavelength and 4) horizontal coherence wavelength of the surrounding magnetization, plus 5) demagnetization radius and 6) demagnetization gradient width.

Fitting results for Martian craters. These predicted circumferential averages are then compared/fitted to circumferentially-averaged radial profiles of both B_{185} and B_{400} for the five largest demagnetized Martian basins: Isidis, Hellas, Utopia, Argyre and the North Polar basin. The multiple altitudes allow useful constraints to be placed on the average magnetization strength, horizontal coherence wavelength and demagnetization radius. Figure 1 demonstrates the fitting results for the Isidis basin, making the assumption of 12 km vertical coherence wavelength. It shows that the mean radius of demagnetization is ~775 km and falls between the largest and smallest topographic rings identified by Frey [5]. The best-fit horizontal coherence wavelength is ~1000 km and the mean bulk magnetization in the assumed 48 km -thick crust is around 1.0 A/m. Similar results are found for the other 4 basins in terms of coherence wavelength, magnetization and the ratio of demagnetization radius to topographic rings.

Conclusions: from other sets of plots like figure 1 and from a comprehensive examination of the relationship between magnetic field, observation altitude, demagnetization radius and horizontal coherence wavelength, we find that:

1) The dominant lateral size of coherently magnetized crust regions is in the range ~325 km to 600 km.

2) The magnetic field observed over a circular demagnetized region is such that clear signatures should only be visible in magnetic field maps at 185 km and 400 km altitude for demagnetization diameters larger than ~600 km and ~1000 km respectively.

3) The ratio of demagnetization diameter to the outer topographic ring diameter is close to 0.8 for the Isidis, Hellas, Argyre and Utopia basins, suggesting that similar basin-forming and shock demagnetization processes occurred in each of these four ancient impacts.

4) If used in conjunction with impact simulations [6] and pressure-demagnetization data for candidate minerals [7], such modeling may lead to improved constraints on the spatial distribution of shock pressure and impact energies needed to form these basins.

References: [1], Hood, L. L. et al., *GRL*, *30*, 2003. [2] Shahnas, H., and J. Arkani-Hamed , *JGR 112*, E02009, 2007, [3] Lillis, RJ et al. *Icarus, 194,* 575-196, 2008. [4] Purucker, M. E., 2008, *Icarus, 197,* 19-23. [5] Frey, H.V. *JGR* 111, E08S91, 2006. [6] Louzada, K.L. and Stewart, S.T., *GRL*, *36*, L15203,

2009. [7] Louzada, K.L. et al., EPSL, submitted, 2009.

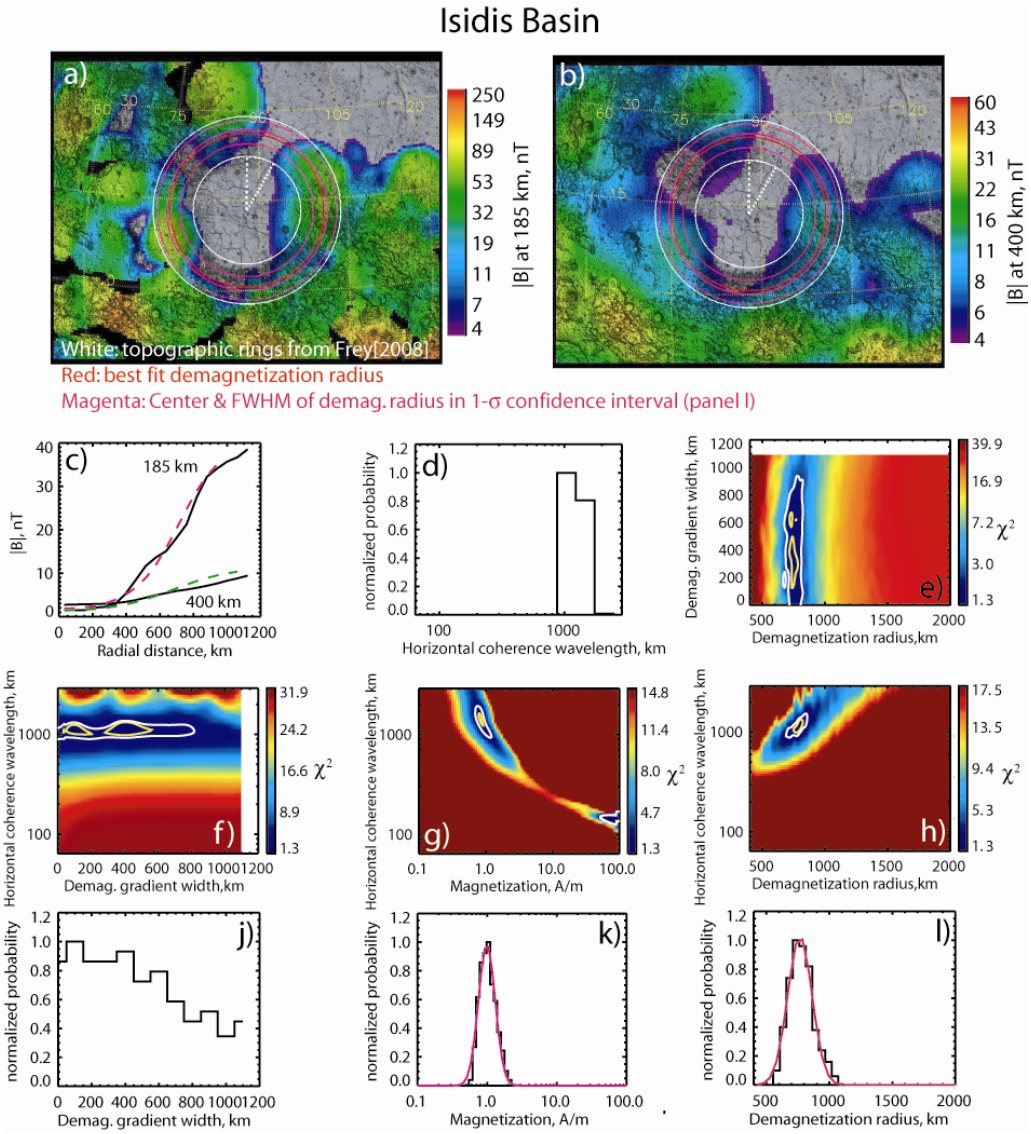

Figure 1: Demagnetization fitting results for the Isidis basin. Panels a) and b) show magnetic field magnitude at 185 km and 400 km respectively. Note the color scales are logarithmic and different. The 3 magenta rings represent the center and FWHM values of the distribution of demagnetization diameter inside the 1-sigma confidence interval (shown in panel l). The white dotted radial lines show the azimuth range over which radial profiles of B_{185} and B_{400} are averaged. These profiles are shown as black lines in panel c), over which the best-fit model predictions are plotted with pink and green dashed lines respectively.

Panel d) shows a histogram of the distribution of values of horizontal coherence wavelength within the 1-sigma confidence interval. Panels e) through l) are arranged symmetrically, with demagnetization gradient width as the abscissa in the left column, magnetization strength in the middle column and demagnetization radius in the right column and horizontal coherence wavelength as the ordinate in the middle row. Panels e) through h) show four different two-dimensional slices of the 4-dimensional χ^2 space defined by demagnetization radius, demagnetization gradient width, magnetization strength and horizontal coherence wavelength. Each 2-d slice correspondents to the χ^2 minimum in the other two dimensions. The white contour corresponds to the 1-sigma confidence interval (i.e. where χ^2 is less than 1.0+min (χ^2)). The yellow contour represents where χ^2 < 0.5 +min (χ^2). The latter contour is not always visible because nearest-neighbor smoothing is applied over each slice for display purposes. Panels j) through l) plot histograms of the distributions of demagnetization gradient, magnetization strength and demagnetization radius inside the 1-sigma confidence interval.